Jordan Journal of Civil Engineering, Volume 8, No. 2, 2014

Prediction of Compressive Strength of Fibrous Composites Using Two Different Approaches

Yousef S. Al Rjoub [1)] and Karim S. Numayr [2)]*

[1)] Civil Engineering Department, Jordan University of Science and Technology, P. O. Box 3030, Irbid, Jordan.
[2)] Dean, Faculty of Engineering , American University of Madaba, P. O. Box 2882, Amman, Jordan.
*Corresponding Author. E-Mail: ysalrjoub@just.edu.jo

ABSTRACT

This paper presents two different approaches to predict the compressive strength of fibrous composites using three-dimensional analysis. These approaches are based on the optimization of compressive stress resulting from the relationship between the compressive stress of the fibrous composite and the shear strength of the matrix material. The first approach is an estimation of compressive strength based on the actual initial misalignment of fibers in the rotated plane. The second approach is an approximation of compressive strength in accordance with the components of the initial fiber misalignment relative to the global axes of the fibrous composite material. The initial fiber misalignment is defined as a curve in the form of a cosine function that has components on the two planes containing the longitudinal axis and defined by initial misalignment angles. Equilibrium equations are then derived for an infinitesimal element along the axis of the fibers using the total potential energy principle. Maximum compressive strength is calculated using the corresponding shear stresses and shear deformations in the matrix, since shear is the dominant mode of failure. The compressive strength corresponding to the shear mode is found to be related to the tangent shear modulus of a fibrous composite material. The two different approaches are used to study the following composites: Carbon/epoxy XAS/914C saturated and dry, Carbon/Peek AS4/PEEK (APC-2), AS4/E7K8, Glass-Vinyl Ester, Glass-Polyester and unidirectional HTS40/977-2. The results obtained in this paper are found to agree well with experimental results and theoretical results available in literature.

KEYWORDS: Carbon fiber, Fibers, Strength, Micro-mechanics, Three-dimensional analysis.

INTRODUCTION AND LITERATURE REVIEW

A micromechanics approach is used in this paper to determine the compressive strength of compression members made of fibrous composites, thereby clarifying the stability state and structural behavior of these members. One of the most important issues to be considered is imperfection of the fibers which occurs during the manufacturing process. Fibers can exhibit different imperfections, such as initial curvature, misalignment and/or initial kinking.

Various micro-mechanical models have been used by different researchers in order to predict the compressive strength of fibrous composites. In a two-dimensional analysis of micro-buckling of fibrous composites, the main mode of failure is considered to be fiber buckling (Rosen, 1965). It is stated that the shear mode, where the fibers are assumed to bend in phase, is the dominant mode rather than the extension mode, where the fibers are assumed to bend out of phase. An initial, sinusoidal deflection of fibers is

Accepted for Publication on 16/1/2014.

assumed by Häberle and Matthews (1994). The shear mode is considered to be the failure mode and the compressive strength of the fibrous composites is proportional to the tangent shear modulus of the shear stress-strain curve of the matrix material. The fibers are considered to be axially incompressible. A two-dimensional micro-mechanical model to predict the compressive strength of unidirectional fibrous composite laminates is proposed by Abu-Farsakh et al. (1997). The fibers are assumed to have initial rotation with no translation at the midpoint, and doubly curved with maximum rotations and translations at the end points. Shear buckling mode is assumed to be the main cause of large shear deformation. The buckling load is determined using the minimum potential energy principle. Four compressive failure modes are suggested by Frost (1992); tensile failure, shear failure, fiber failure and fiber compressive failure. All modes depend on the fiber volume fraction and the mechanical properties of the fibers and the matrix. Four mechanisms of failure are identified by Jelf and Fleck (1995); fiber failure, elastic micro-buckling, matrix failure and plastic micro-buckling. It is found that plastic micro-buckling is the dominant compressive failure in polymeric matrix composites. In the Yeh and Teply (1990) model, the predicted compressive strength is found to be suitable for composites with a very large shear modulus, while local fiber misalignment affects the compressive strength of Kevlar/Epoxy composites. Soutis and Fleck (1990) developed a theoretical model to predict the static strength of notched laminates and carried out an experiment on carbon/epoxy, T800/924C, composite laminates with circular holes, to determine the compressive failure stress. They find that matrix cracking initiates failure and micro-buckling of the fiber occurred at the edges of the hole, since high in-plane compressive stresses are developed. In a study by Wisnom (1990), the compressive strength of fibrous composites is estimated using a model that assumes the fibers to be straight and parallel to one another, with an initial angle of rotation with respect to the axis of loading. It is concluded that shear instability in the matrix material reduces the compressive strength considerably. A mathematical model has been developed by Budiansky (1983) to predict the compressive strength of fibrous composites considering fiber misalignment, yield stress and shear in the matrix material in the kink band. Fleck and Budiansky (1990) and Budiansky and Fleck (1993) have considered plastic micro-buckling, while neglecting fiber bending in their analysis. Steif (1990, 1990) has assumed that fiber kinking is associated with fiber breakage due to buckling of the composite material. A bundle of fiber breaks are observed at a critical strain comparable to compressive strength, which leads to the conclusion that fiber breaks are the limiting step in kink band formation. It has been postulated by Yurgartis (1987) that real fiber misalignments are in and out of plane with the laminate. This agrees with misalignment patterns in carbon fibrous composites found by Creighton et al. (2001) using a special image analysis algorithm. Karakuzu et al. (2010) carried out an experimental work to study the behavior of a glass/ epoxy laminated composite plate subjected to traction forces by four pins. They considered the edge distance from the hole, longitudinal and transverse distances between holes and the pin diameter in their analysis. Ranganatahn and Mantena (2003) have studied the effect of hybridization of buckling characteristics of flat pultruded glass-graphite/epoxy beams using Euler's formulation, finite element modeling and experimentation and have found that hybridization improves the buckling performance of composite beams. Huang (2001) has developed a micromechanical bridging model to determine the properties of unidirectional and multidirectional lamina such as: thermoelastic, elasto-plastic, ultimate failure strength, strength at high temperature, fatigue strength and an S-N curve. An analytical model, based on experimentally obtained compressive strengths and inverse micro-mechanical models, has been developed by Mishra and Naik (2009) to define elastic properties of transversely isotropic fibers. An experimental work

has been conducted by Chen et al. (2006) to study the behavior of IM7/8551-7 Graphite Epoxy laminates subjected to in-plane biaxial compression. It has been concluded that their results agree well with the Mohr-Coulomb shear failure law when applied to the fibers, but not to the matrix. It has also been concluded that fiber shearing is the dominant failure mechanism for this material for all laminates orientations and biaxiality ratios. Huang (2001) has also developed a micro-mechanical strength theory to estimate the ultimate strength of unidirectional fiber reinforced composites. This theory considers the fibers to be transversely isotropic in the elastic region and isotropically hardened in the plastic region. Constituent properties and fiber volume fraction are used as input data and a bridging matrix is used to correlate the stresses in the fibers with those in the matrix. The stress level at failure in each constituent and the failure mode are defined. A simple formula was proposed by Barbero (1998) and Tumblin and Barbero (1996) to estimate the compressive strength of unidirectional polymer matrix that can be used in the design of parts made of such composites. It requires the following parameters that can be defined by well-established techniques: shear stiffness, strength and standard deviation of fiber misalignment. A damage mechanics model based on a Gaussian distribution of fiber misalignment for the prediction of compressive strength of fibrous composites using material parameters measured by reliable methodologies is proposed by Barbero and Tomblin (1996). Predicted values of compressive strength for eleven different F-glass reinforced pultruded composites are found to be in good agreement with experimental ones. A graphical method similar to that used by Budiansky (1983) is used by Jumahat et al. (2011) to predict the compressive strength of unidirectional Carbon fiber reinforced polymer composite laminates. It is based on the shear stress-strain curve of the fiber-matrix laminate rather than the shear stress-strain of the matrix material. It takes into account the additional compressive strength of the post buckling mode after kinking of fibers and associated yielding in shear of the matrix. The results for HTS40/977-2 and the failure mechanism have been verified experimentally using scanning electron microscopy (SEM) and optical microscopy. A similar mechanism, that is; starting by bending of misalignment fibers then forming a kink band after two breakages occurred and later a failure of the matrix, was illustrated by Berbinau et al. (1999) for 0° unidirectional carbon-fiber-reinforced plastic. It was concluded that fibers cannot fail in tension on their convex side but rather fail in compression on their concave side.

Two approaches based on a three-dimensional micro-mechanical model are developed herein to predict the maximum buckling load and, thus, the compressive strength of fibrous composite materials. A continuous displacement cosine function that satisfies continuity conditions is proposed to define the imperfect fibers before and after deformation. Equilibrium equations of a matrix-fiber infinitesimal element are derived using the total potential energy principle and then are simplified using the proposed displacement field. The critical buckling load is then defined in terms of matrix shear strength and the initial misalignment of fibers. The compressive strength is estimated for some fiber-reinforced composites and is compared to available experimental data and the results of other models available in literature.

MODEL DERIVATION

A representative volume of a fibrous composite in three-dimensional space is shown in Figure 1. It is composed of a curved fiber of length l and diameter d_f, embedded in a matrix of widths t_y and t_z, in y- and z-directions, respectively. The material is assumed to be macroscopically orthotropic, homogeneous and initially stress-free. The position vector from the origin to any point on the space curve, which represents the initial waviness of fibers, is given by:

$$\mathbf{r} = C_0 x\mathbf{i} + A_0 \cos\frac{\pi x}{l}\mathbf{j} + B_0 \cos\frac{\pi x}{l}\mathbf{k} \qquad (1)$$

As illustrated in Figure 2, A_0 and B_0 are the amplitudes of the initial wave in the *y*- and *z*-directions, respectively. The space curve is assumed to make only one pitch, of length *l*, along the *x*-axis, leading to C_0 =1 in Equation (1). The proposed space curve and corresponding position vector satisfy the location of the tips ($\mathbf{r} = \frac{l}{2}\mathbf{i} @ x = \frac{l}{2}$ and $\mathbf{r} = -\frac{l}{2}\mathbf{i} @ x = -\frac{l}{2}$) and midpoint of the fiber ($\mathbf{r} = (A_0 j + B_0 k) @ x = 0$). The position vector after fiber deformation is given by:

$$\mathbf{R} = Cx\mathbf{i} + A\cos\frac{\pi x}{l}\mathbf{j} + B\cos\frac{\pi x}{l}\mathbf{k} \quad (2)$$

where *A* and *B* are amplitudes in the y- and z-directions, respectively, and $C = 1-(u-u_0)$. The displacement vector ($\boldsymbol{\delta} = \mathbf{R} - \mathbf{r}$) is given by:

$$\boldsymbol{\delta} = (u-u_o)\mathbf{i} + (v-v_o)\mathbf{j} + (w-w_o)\mathbf{k} \quad (3)$$

where,

$$\left.\begin{aligned} u-u_o &= (A-A_0)x \\ v-v_o &= (A-A_0)\cos\frac{\pi x}{l} \\ w-w_o &= (B-B_0)\cos\frac{\pi x}{l} \end{aligned}\right\} \quad (4)$$

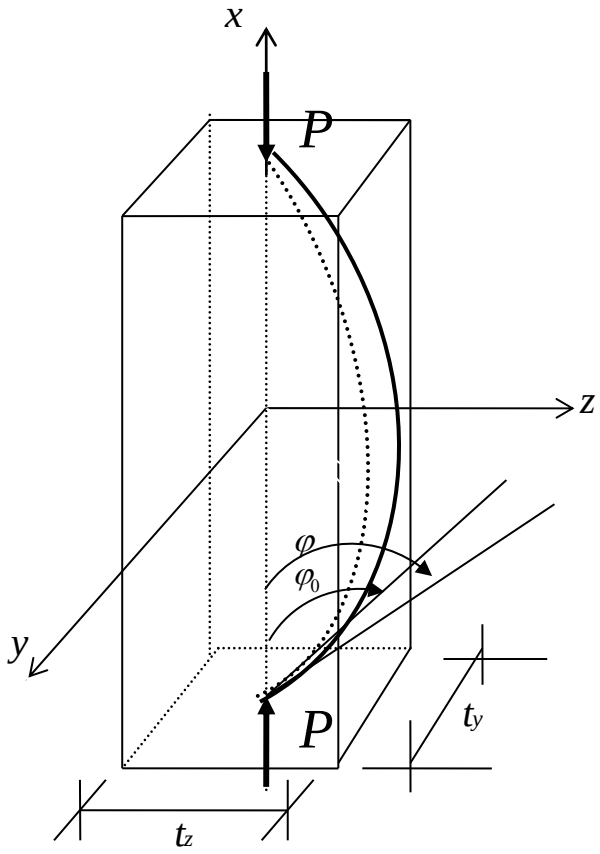

Figure (1): Representative volume of the present model

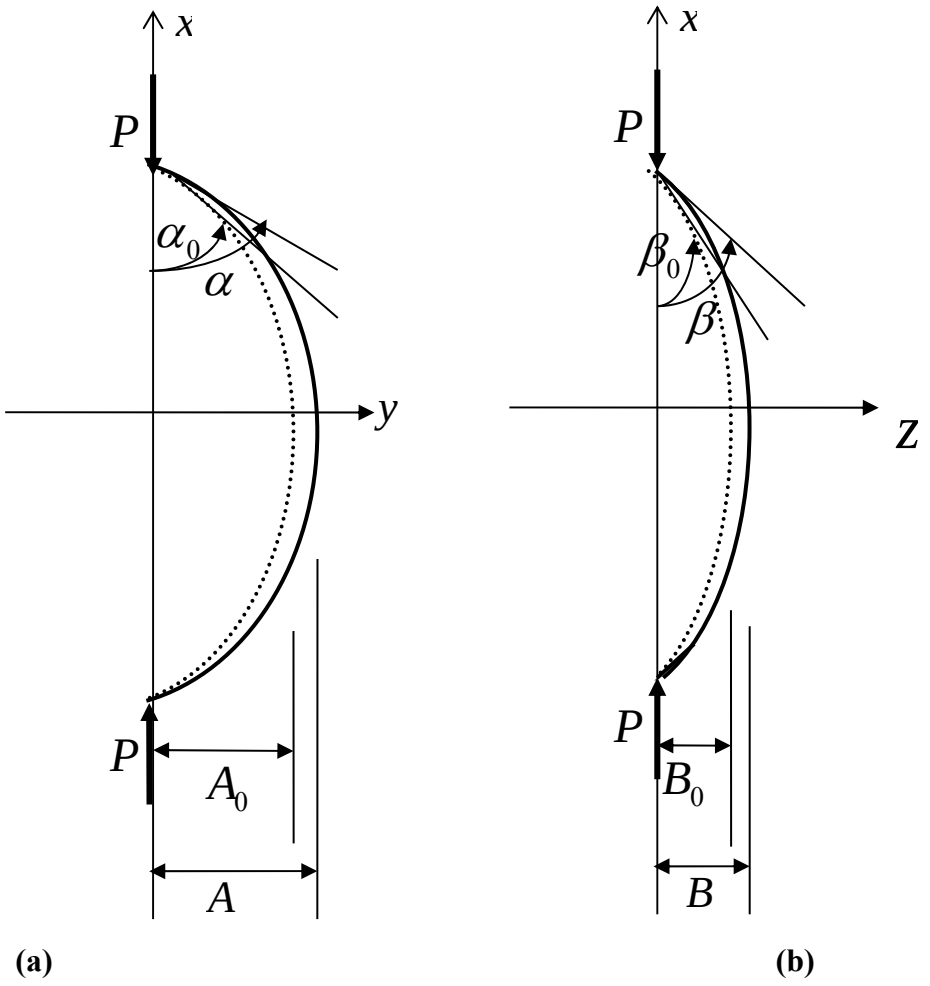

Figure (2): Projection of deformed fiber before and after loading in (a)x-y plane; (b) x-z plane

are the deformation components of the fiber in the x-, y- and z- directions, respectively. The following partial derivatives, $\frac{\partial u}{\partial y}=\frac{\partial v}{\partial y}=\frac{\partial w}{\partial y}=\frac{\partial u}{\partial z}=\frac{\partial v}{\partial z}=\frac{\partial w}{\partial z}=0$, according to the assumed deformation of fibers. The angles between the fiber and the *x*-axis can be expressed in terms of amplitudes before and after loading. The components of these angles in the *x*-*y* and *x*-*z* planes are defined as follows: $\alpha_0=\frac{\pi}{l}A_0$, $\alpha=\frac{\pi}{l}A$, $\beta_0=\frac{\pi}{l}B$ and $\beta=\frac{\pi}{l}B$.

Using the total potential energy principle, the strain energy of the fibrous composite is given by:

$$U=\int_V\left(\int_{\kappa_y} M_z d\kappa_y+\int_{\kappa_z} M_y d\kappa_z+\int_{\gamma_{xy}} \tau_{xy} d\gamma_{xy}+\int_{\gamma_{xz}} \tau_{xz} d\gamma_{xz}\right)dV \qquad (5)$$

where, $M_z = -E_f I_f \frac{d^2}{dx^2}(v - v_0)$, $M_y = -E_f I_f \frac{d^2}{dx^2}(w - w_0)$

and E_f and I_f are the modulus of elasticity and moment of inertia of the fiber, respectively; κ_y, κ_z are the curvatures in the x-y plane and in the x-z plane, respectively.

Neglecting the bending terms of the fiber, and noting that the moment of inertia of the fiber I_f is very small, Equation (5) reduces to:

$$U = \left(\int_{-l/2}^{l/2} \left(\int_0^{\gamma_{xy}} \tau_{xy} d\gamma_{xy} + \int_0^{\gamma_{xcz}} \tau_{xz} d\gamma_{xz} \right) dx \right) dydz \quad (6)$$

The potential energy of the externally applied forces is given by:

$$V = \left(\int_{-l/2}^{l/2} \sigma_c \frac{du}{dx} dx \right) dydz \quad (7)$$

where, $\frac{du}{dx} = -\frac{1}{2}\left(\frac{dv}{dx}\right)^2 - \frac{1}{2}\left(\frac{dw}{dx}\right)^2$

The total potential energy is given by:

$$\pi = U + V \quad (8)$$

which can be written, after substitution of Equation (6) and $\frac{du}{dx}$ into Equation (7), as:

$$\pi = \int_A \left[\int_{-l/2}^{l/2} \left(\int_0^{\gamma_{xy}} \tau_{xy} d\gamma_{xy} + \int_0^{\gamma_{xz}} \tau_{xz} d\gamma_{xz} - \frac{1}{2}\sigma_c \gamma_{xy}^2 - \frac{1}{2}\sigma_c \gamma_{xz}^2 \right) dx \right] dA \quad (9)$$

Minimization of the total potential energy with respect to γ_{xy}, $\frac{\partial \pi}{\partial \gamma_{xy}} = 0$, yields the following:

$$\int_A \int_{-l/2}^{l/2} \left(\tau_{xy} - \sigma_c \gamma_{xy} \right) dx dA = 0 . \quad (10)$$

Equation (10) yields the following equilibrium equation in the x-y plane:

$$\tau_{xy} - \sigma_c \gamma_{xy} = 0 \quad (11)$$

and implies that $\sigma_c = G\left(\gamma_{xy}\right)$.

Similarly, minimization of the total potential energy with respect to γ_{xz} yields the following equilibrium equation in the x-z plane:

$$\tau_{xz} - \sigma_c \gamma_{xz} = 0 \quad (12)$$

which implies $\sigma_c = G\left(\gamma_{xz}\right)$.

The nonlinear shear stress-strain relationships of the composite material are: $\tau_{xy} = G(\gamma_{xy})\,\gamma_{xy}$, and $\tau_{xz} = G(\gamma_{xz})\,\gamma_{xz}$,

where, $G(\gamma_{xy})$ and $G(\gamma_{xz})$ are the secant shear modulus at γ_{xy} and γ_{xz} shear strains, respectively. Applying the strain-displacement relationship, the shear strain can be expressed as: $\gamma_{xy} = -\pi \frac{(A - A_0)}{l} \sin\frac{\pi x}{l}$, and $\gamma_{xz} = -\pi \frac{(B - B_0)}{l} \sin\frac{\pi x}{l}$.

In the x-y plane for $B_0 = 0$ and $\beta_0 = 0$, the maximum compressive strength is:

$$(\sigma_{c\max})_y = \frac{\tau_{xy}}{\gamma_{xy} + \alpha_0} . \quad (13)$$

In the x-z plane for $A_0 = 0$ and $\alpha_0 = 0$, the maximum compressive strength is:

$$(\sigma_{c\max})_z = \frac{\tau_{xz}}{\gamma_{xz} + \beta_0} . \quad (14)$$

These equations are derived after substitution of dv/dx and dw/dx, neglecting the M_y and M_z terms, and proving that the maximum compressive strength values are simply $G(\gamma_{xy})$ in Equation (13) and $G(\gamma_{xz})$ in Equation (14), as discussed in (Häberle and Matthews, 1994) and derived in this study. These equations indicate that the maximum compressive stress can be obtained using the tangent of the shear stress-strain curve at the shear strain where instability occurs.

The first approach is based on the direct calculation of the maximum compressive stress for the proposed deformed shape of the fiber, Figure (2), which can be used for the case of similar shear stress- strain curves in the x-y and x-z planes according to the following formula:

$$\sigma_{c\max} = \frac{\tau}{\gamma + \varphi_0}, \tag{15}$$

where τ, γ are, respectively, the shear stress and shear strain in the matrix for the proposed deformed curve of the fiber. φ_0 is the initial misalignment angle of the deformed shape of the fiber, which is defined by the initial misalignment angles in the x-y plane, α_0, and in the x-z plane, β_0, and given by the following formula:

$$\phi_0 = \sqrt{\alpha_0^2 + \beta_0^2}\ . \tag{16}$$

The second approach is based on the maximization of σ_c in the following quadratic expression, which is the magnitude of the zero vector having components in the y- and z- directions, Equations (11) and (12):

$$(\tau_{xy} - \sigma_c \frac{dv}{dx})^2 + (\tau_{xz} - \sigma_c \frac{dw}{dx})^2 = 0 \tag{17}$$

Accordingly, the minimization of compressive strength with respect to γ_{xy}, we obtain::

$$\left(\sigma_{c\max}\right)_y = \frac{(\gamma_{xy}^* + \alpha_0)\tau_{xy}^* + (\gamma_{xz} + \beta_0)\tau_{xz}}{(\gamma_{xy}^* + \alpha_0)^2 + (\gamma_{xz} + \beta_0)^2}, \tag{18}$$

where $\gamma_{xy}^*, \tau_{xy}^*$ are, respectively, the shear strain and shear stress in the x-y plane for a given value of α_0 and are found from Figure 3, using $-\alpha_0$ instead of $-\varphi_0$.

And, with respect to γ_{xz}, we obtain:

$$\left(\sigma_{c\max}\right)_z = \frac{\left(\gamma_{xy} + \alpha_0\right)\tau_{xy} + \left(\gamma_{xz}^* + \beta_0\right)\tau_{xz}^*}{\left(\gamma_{xy} + \alpha_0\right)^2 + \left(\gamma_{xz}^* + \beta_0\right)^2}\ . \tag{19}$$

where $\gamma_{xz}^*, \tau_{xz}^*$ are, respectively, the shear strain and shear stress in the x-z plane for a given value of β_0 and are found from Figure 3, using $-\beta_0$ instead of $-\varphi_0$.

$\left(\sigma_{c\max}\right)_y$ and $\left(\sigma_{c\max}\right)_z$ are evaluated using the solution procedure discussed in the following section of this paper. The maximum compressive stress is estimated using least square approximation:

$$\sigma_{c\max} = \sqrt{\frac{\left(\sigma_{c\max}\right)_y^2 + \left(\sigma_{c\max}\right)_z^2}{2}}\ . \tag{20}$$

METHOD OF SOLUTION

First Approach

Given the values of α_0 and β_0, the misalignment angle, φ_0 is calculated from Equation (16). A shift, by an amount φ_0, is taken in the negative direction of the abscissa, γ_axis, in the shear stress- strain curve of the matrix. A tangent curve is drawn such that it passes through the point $(-\varphi_0)$ on the γ_axis. The shear stress and shear strain values corresponding to the tangent point at the curve are obtained. The value of the maximum compressive strength is evaluated using Equation (15). This method of solution is illustrated in Figure (3).

Second Approach

For given values of α_0 and β_0, the value of maximum stress of fibrous composite is estimated according to the following solution procedure. First, the values of γ_{xy}^* and τ_{xy}^* are found using graphical determination of the tangent point, as discussed previously, for a shift in the abscissa axis, γ_{xy} equal to $(-\alpha_0)$. Second, the values of τ_{xz} are obtained from the shear stress-strain curve of the matrix material for values of γ_{xz} between 0.01 and 0.06. Third, the values of $\left(\sigma_{c\max}\right)_y$ are calculated from Equation (18) and are plotted for values of γ_{xz} from 0.01 to 0.06. Fourth, the value of $\left(\sigma_{c\max}\right)_y$ is defined as the maximum value on the $\left(\sigma_{c\max}\right)_y$ - γ_{xz} plotted curve, Figure (4). The same four previous steps are repeated for a shift of $(-\beta_0)$ to evaluate γ_{xz}^* and τ_{xz}^*, τ_{xy} is obtained for values of γ_{xy} between 0.01 and 0.06. The values of $\left(\sigma_{c\max}\right)_z$ are calculated from Equation (19) and are plotted for the different values of γ_{xy} from 0.01 to 0.06, and the value of $\left(\sigma_{c\max}\right)_z$ is defined as the maximum value on the $\left(\sigma_{c\max}\right)_z$ - γ_{xy} curve. Finally, the compressive strength of the fibrous composite material in consideration is estimated using a least squares approximation, Equation (20).

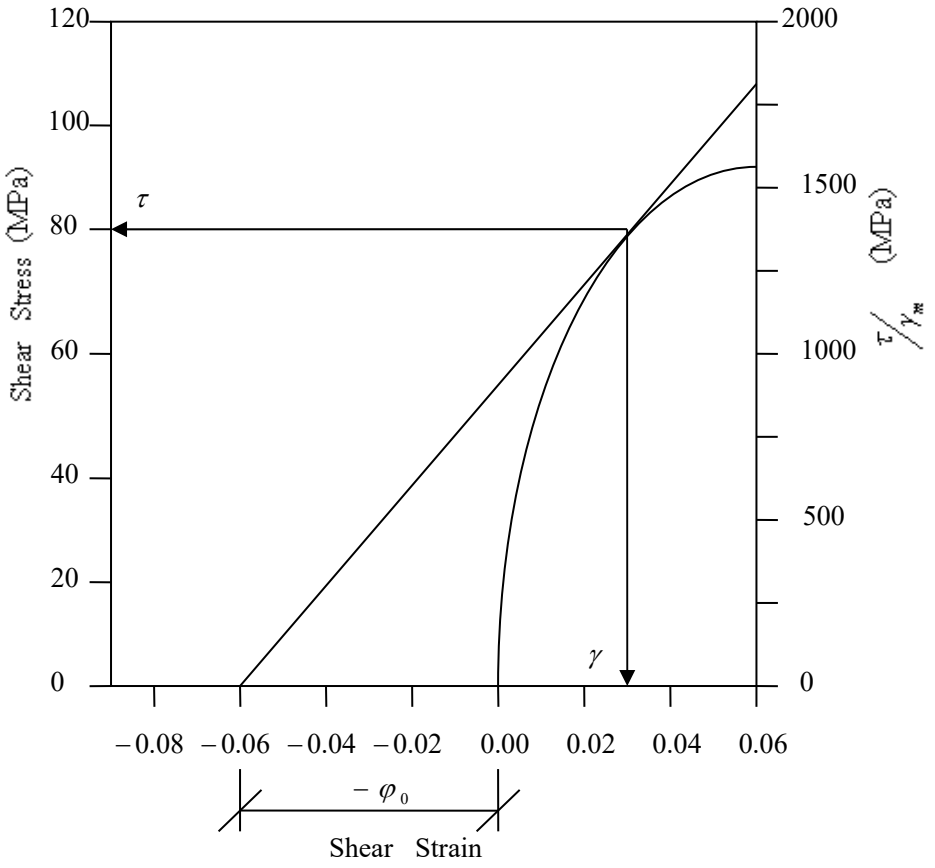

Figure (3): A representative curve for matrix material showing the tangential line method

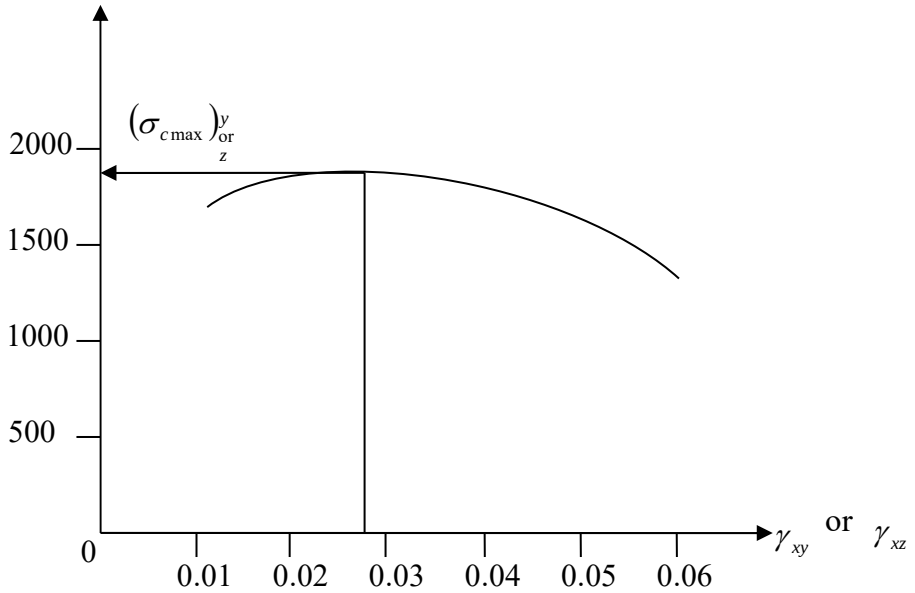

Figure (4): The maximum compressive stress $(\sigma_{c\max})_y$ or $(\sigma_{c\max})_z$ *versus* shear stress γ_{xy} or γ_{xz}

RESULTS AND DISCUSSION

The three-dimensional micromechanical model and the two different solution approaches are examined for the following different fibrous composite materials; XAS/914 C 'Saturated', XAS/914C 'Dry', AS4/PEEK 'APC-2', AS4/E7K8, Glass-Vinyl Ester, Glass-Polyester and unidirectional HTS40/977-2. Engineering and geometric properties of these materials, shown in Table 1, and the shear stress-strain curve, used to establish the results in this study, are taken from (Abu Farsakh et al., 1997; Jumahat et al., 2011; Berbinau et al., 1999). The maximum compressive stresses are estimated using the two approaches for different values of initial misalignment angles α_0 and β_0. A value of $\alpha_0 = 1^\circ$ is used for XAS/914C 'Saturated' and XAS/914C 'Dry', a value of $\alpha_0 = 1.25^\circ$ is used for AS4/PEEK 'APC-2', a value of $\alpha_0 = 1.2^\circ$ is used for AS4/E7K8, a value of $\alpha_0 = 3.3^\circ$ is used for Glass-Vinyl Ester, a value of $\alpha_0 = 3.4^\circ$ is used for Glass-Polyester, a suggested value of $\alpha_0 = 1^\circ$ is used for UD HTS40/977-2, and different values of β_0 are used. In this study, the values of α_0 used for the different fibrous composites are chosen according to measured or estimated values available in literature, see (Häberle and Matthews, 1994; Barbero, 1998), while the values of β_0, which are not available in literature, are taken to be in the range of 0° to 2.25°.

The value of compressive stress is estimated according to the first and second approaches, Equations (15) and (20), for different values of $\phi_0 = \sqrt{\alpha_0^2 + \beta_0^2}$, which are listed in Tables 2,3 and 4, and compared to experimental values (Häberle and Matthews, 1994) and theoretical models (Rosen, 1965; Häberle and Matthews, 1994) available in literature. Table 2 includes a list of the compressive strengths of XAS/914C 'Saturated' for a value of $\alpha_0 = 1^\circ$, β_0 and, thereby, ϕ_0. It can be seen that the results obtained from the present first approach in this study are in good agreement with the experimental ones from (Häberle and Matthews, 1994) for an initial misalignment angle $\phi_0 \sim 1^\circ$. It can also be observed that the results obtained from the present second approach approximate the experimental value at initial misalignment angles $\alpha_0 = 1^\circ$ and $\beta_0 \sim 0.54^\circ$. Therefore, the present three-dimensional analysis using a cosine function for initial curvature of the fiber suggests an initial misalignment angle of 1° in one direction and 0.0°, according to the present first approach, and 0.54°, according to the present second approach, in the other direction. The compressive strength value obtained by model (Rosen, 1965) overestimates the experimental value because the two-dimensional model (Rosen, 1965) assumes that the compressive strength is proportional to the elastic shear modulus. The percentage difference from the experimental value for the present first approach is -1% and is 3.3% for the present second approach, when $\beta_0 = 0^\circ$. It can be concluded that the present first approach yields better results than the present second approach, since the present first approach is an estimate of the compressive strength for the actual initial misalignment angles of fibers in the rotated plane rather than the global axes of fibrous composites. The first and second approaches of the present study are examined for XAS/914C 'Dry' and AS4/PEEK 'APC-2'. Values of $\sigma_{c\max}$ are listed in Tables 3 and 4. A value of $\sigma_{c\max} = 1790$ MPa is predicted for $\varphi_0 = 1^\circ$ according to the present first approach and a value of $\sigma_{c\max} = 1905$ MPa is predicted at $\alpha_0 = 1^\circ$ and $\beta_0 = 0^\circ$ according to the present second approach, compared to an experimental value of 1800 MPa for XAS/914C 'Dry'. The percentage difference from the experimental value of 1800 MPa for the present first approach is -0.55% and for the present second approach is 5.83% when using $\beta_0 = 0^\circ$. Again, model (Rosen, 1965) overestimates the maximum compressive strength for this material. The difference of the results obtained by the two present approaches and those obtained by analytical models (Häberle and Matthews, 1994; Barbero, 1998) is due to the fact that the model used in this paper is three-dimensional, taking into account the actual initial misalignment angle of fibers in the rotated

plane and in the global axes of fibrous composite; while the models from (Häberle and Matthews, 1994; Barbero, 1998) are according to a two-dimensional analysis. Also, $\sigma_{c\max}$ predicts the experimental value of 1500 MPa for $\phi_0 \sim 1.25^\circ$ according to the present first approach and $\alpha_0 = 1.25^\circ$ and $\beta_0 \sim 0.73^\circ$ according to the present second approach for AS4/PEEK 'APC-2'. The percentage difference from the experimental value for the present first approach is -0.67% and is 4.67% for the present second approach at $\beta_0 = 0^\circ$. Again, for this material, the results obtained by model (Rosen, 1965) give an overestimate of the compressive strength. The compressive strength value of 1490 MPa obtained by model (Häberle and Matthews) at $\alpha_0 = 1.25^\circ$, based on the mean of distribution of absolute fiber angles, MDAFA, is in good agreement with the experimental value, while the value of 1295 MPa, obtained at $\alpha_0 = 1.53^\circ$, based on the standard deviation of transformed distribution of fiber angles, SDTDFA, underestimates the experimental value.

Table 1. Engineering and geometric properties of fibrous composite materials

Property	Fibrous Composite						
	XAS/914C 'saturated'	XAS/914C 'dry'	AS4/PEEK 'APC-2'	AS4/E7K8	Glass-Vinyl Ester	Glass-Polyester	HTS40/977-2
G (GPa)	4.75	5	5.5	NA	NA	NA	NA
G_m (Gpa)	2.27	2.4	2.55	NA	2.35	2.35	NA
E_f (GPa)	235	235	220	241	72.35	72.35	239
d_f (μm)	7	7	7	7	13	13	7
L (m)	0.01	0.01	0.01	NA	NA	NA	NA
V_f	0.58	0.58	0.61	0.60	0.43	0.40	0.58

G: Effective shear modulus, G_m: Matrix shear modulus, E_f: Longitudinal Young's modulus of fiber, V_f: Fiber volume fraction.

Table 2. Compressive strength of XAS/914C 'saturated', $\alpha_0 = 1^\circ$

φ_0 (deg.)	β_0 (deg.)	Present Eqn. (15) σ_{cmax} (MPa)	Present Eqn. (20) σ_{cmax} (MPa)	Model (Häberle and Matthews, 1994) $\sigma_{c\max}$ (MPa) Based on SDTDFA	Model (Häberle and Matthews, 1994) $\sigma_{c\max}$ (MPa) Based on MDAFA	Model (Rosen, 1965) σ_{cmax} (MPa)	Exp. Result (Häberle and Matthews, 1994) (MPa)
1	0	1480	1550	1470	1650	5400	1500
1.03	0.25	1470	1540				
1.12	0.5	1400	1510				
1.25	0.75	1350	1435				
1.41	1	1280	1365				

The compressive strength values for different initial misalignment angles are estimated using the first and second approaches of this study and compared to values available in literature for other fibrous composites, namely; AS4/E7K8, Glass-Vinyl Ester, Glass-Polyester and unidirectional HTS40/977-2, see Tables 5, 6, 7 and 8. The compressive strength values of AS4/E7K8 are listed in Table 5. As can be seen, the values 1670 MPa, and 1685 MPa, according to approximate and explicit formulae of (Barbero, 1998),

agree well with the experimental one of (Tomblin and Barbero, 1996). Also, it can be seen from the results that the present first approach yields the experimental value at $\phi_0 \sim 1.39^\circ$, while the present second approach yields the experimental value at $\alpha_0 = 1.2^\circ$ and $\beta_0 = 1.05^\circ$. The percentage difference from the experimental value for the present two approaches is 25.6% and 40.7%, respectively, when neglecting the misalignment in the opposing direction. The values of approximate and explicit formulae of (Barbero, 1998) and the experimental value of (Barbero and Tomblin, 1996) of about 522 MPa for Glass-Vinyl Ester with an initial misalignment angle of 3.3° agree well with the present first approach for an initial misalignment angle $\phi_0 \sim 4.11^\circ$ and with the present second approach for $\alpha_0 = 3.3^\circ$ and $\beta_0 \sim 1.7^\circ$, see Table 6. The percentage difference from the experimental value for the present first approach is 22.61% and is 39.85% for the present second approach, at $\beta_0 = 0^\circ$. For Glass-Polyester, Table 7, the compressive strength value of about 370 MPa according to the approximate and explicit formulae of (Barbero, 1998) underestimates the experimental value obtained by (Barbero and Tomblin, 1996). The experimental value of 478 MPa agrees with the present first approach for $\phi_0 = 3.4^\circ$ and with the present second approach for $\alpha_0 = 3.4^\circ$ and $\beta_0 = 1.22^\circ$.

Table 3. Compressive strength of XAS/914C 'dry', $\alpha_0 = 1^\circ$

φ_0 (deg.)	β_0 (deg.)	Present Eqn. (15) σ_{cmax} (MPa)	Present Eqn. (20) σ_{cmax} (MPa)	Model (Barbero, 1998) $\sigma_{c\,max}$ (MPa)		Model (Häberle and Matthews, 1994) $\sigma_{c\,max}$ (MPa)		Model (Rosen, 1965) σ_{cmax} (MPa)	Exp. Result (Häberle and Matthews, 1994) (MPa)
				Approximate formula	Explicit formula	Based on SDTDFA	Based on MDTDFA		
1	0	1790	1905	1762	1705	1775	1970	5710	1800
1.03	0.25	1760	1900						
1.12	0.5	1730	1895						
1.25	0.75	1560	1830						
1.41	1	1470	1750						

Table 4. Compressive strength of AS4/PEEK 'APC-2', $\alpha_0 = 1.25^\circ$

φ_0 (deg.)	β_0 (deg.)	Present Eqn. (15) σ_{cmax} (MPa)	Present Eqn. (20) σ_{cmax} (MPa)	Model (Häberle and Matthews, 1994) $\sigma_{c\,max}$ (MPa)		Model (Rosen, 1965) σ_{cmax} (MPa)	Exp. Result (Häberle and Matthews, 1994) (MPa)
				Based on SDTDFA	Based on MDAFA		
1.25	0	1490	1570	1295	1490	6071	1500
1.27	0.25	1480	1560				
1.35	0.5	1420	1535				
1.46	0.75	1360	1495				
1.6	1	1290	1425				

Table 5. Compressive strength of AS4/E7K8, $\alpha_0 = 1.2^\circ$

φ_0 (deg.)	β_0 (deg.)	Present Eqn. (15) σ_{cmax} (MPa)	Present Eqn. (20) σ_{cmax} (MPa)	Model (Barbero, 1998)		Exp. Result (Tomblin and Barbero, 1996) (MPa)
				Approximate formula $\sigma_{c\,max}$ (MPa)	Explicit formula $\sigma_{c\,max}$ (MPa)	
1.2	0	2120	2375	1670	1685	1688
1.23	0.25	2025	2320			
1.3	0.5	1870	2200			
1.42	0.75	1630	1980			
1.56	1.0	1410	1740			
1.73	1.25	1190	1480			

Table 6. Compressive strength of Glass-Vinyl Ester, $\alpha_0 = 3.3^\circ$

φ_0 (deg.)	β_0 (deg.)	Present Eqn. (15) σ_{cmax} (MPa)	Present Eqn. (20) σ_{cmax} (MPa)	Model (Barbero, 1998)		Exp. Result (Barbero and Tomblin, 1996) (MPa)
				Approximate formula $\sigma_{c\,max}$ (MPa)	Explicit formula $\sigma_{c\,max}$ (MPa)	
3.3	0	640	730	498	506	522
3.31	0.25	635	725			
3.34	0.5	620	715			
3.38	0.75	600	700			
3.45	1.0	540	660			
3.53	1.25	520	615			
3.62	1.50	500	560			
3.74	1.75	465	500			

Table 7. Compressive strength of Glass-Polyester, $\alpha_0 = 3.4^\circ$

φ_0 (deg.)	β_0 (deg.)	Present Eqn. (15) σ_{cmax} (MPa)	Present Eqn. (20) σ_{cmax} (MPa)	Model (Barbero, 1998)		Exp. Result (Barbero and Tomblin, 1996) (MPa)
				Approximate formula $\sigma_{c\,max}$ (MPa)	Explicit formula $\sigma_{c\,max}$ (MPa)	
3.4	0	480	540	370	374	478
3.41	0.25	477	535			
3.44	0.5	475	528			
3.48	0.75	470	515			
3.54	1	460	500			
3.62	1.25	445	480			
3.72	1.5	430	460			

Table 8. Compressive strength of UD HTS40/977-2, $\alpha_0 = 1^\circ$

φ_0 (deg.)	β_0 (deg.)	Present Eqn. (15) σ_{cmax} (MPa)	Present Eqn. (20) σ_{cmax} (MPa)	Model (Jumahat et al., 2011) σ_{cmax} (MPa)			Model (Berbinau et al., 1999) σ_{cmax} (MPa)	Model (Budiansky, 1983) σ_{cmax} (MPa)	Exp. Result (Jumahat et al., 2011) (MPa)
				Combined modes model	Fiber microbuckling	Fiber kinking			
1	0	1480	1730	1334	1059	1588	750	1000	1396
1.03	0.25	1425	1675						
1.12	0.5	1370	1625						
1.25	0.75	1315	1575						
1.41	1	1250	1500						
1.6	1.25	1175	1420						
1.8	1.5	1100	1340						
2.02	1.75	990	1240						
2.24	2	890	1120						
2.46	2.25	890	1000						

The percentage difference from the experimental value of this material is 0.41% based on the present first approach and is 12.97% based on the present second approach, when $\beta_0 = 0^\circ$. For the unidirectional HTS40/977-2 composite material, a suggested value of $\alpha_0 = 1^\circ$ is used. The values of compressive strength are listed in Table 8. The value of 1334 MPa for an initial misalignment angle of 2° predicted in (Jumahat et al., 2011), taking into account the additional strength provided by the matrix after the formation of a kink band, agrees well with the experimental value. An experimental value of 1396 MPa has been measured by (Jumahat et al., 2011). This value agrees with the present first approach at $\phi_0 \sim 1.06^\circ$ and with the present second approach at $\alpha_0 = 1^\circ$ and $\beta_0 \sim 1.32^\circ$. The value 750 MPa from (Berbinau et al., 1999) underestimates the compressive strength because it does not take into account the additional strength provided by the matrix after the formation of the kink band. Bearing in mind that the actual initial misalignment angle is about 2°, the present first approach value is in good agreement with that of (Budiansky, 1983), 1000 MPa, for $\phi_0 = 2^\circ$ as well as the present second approach value for $\alpha_0 = 1^\circ$ and $\beta_0 \sim 2.25^\circ$.

CONCLUSIONS

Two approaches are developed in the present study to estimate the compressive strength of fibrous composites using a three-dimensional micromechanical model having a cosine function representing the initial curvature of the fibers. It is found that the initial misalignment of fibers excites the dominant shear failure mode of the matrix, accompanied with the non-linear shear stress-strain relationship of the matrix material, the compressive strength is determined accordingly. In addition, the shape of the initial misalignment of the fibers plays a vital role in the determination of the compressive strength of fibrous composites. The two approaches are validated for several fibrous composite materials. The two approaches used herein are found to be useful in a

three-dimensional analysis, and lead to reliable results that are in good agreement with experimental data.

Acknowledgement

The authors convey their sincere gratitude to Doctor Kirsten McKay for editing the manuscript.

REFERENCES

Abu-Farsakh, G. A., Numayr, K. S., and Hamad, K. A. (1997). "A micro-mechanical model for predicting the compressive strength of fibrous composite materials". Composite Science Technology, 57, 9-10.

Barbero, E. J. (1998). "Prediction of compression strength of unidirectional polymer matrix composites". Journal of Composite Materials (March), 32 (5), 483-502.

Barbero, E. J., and Tomblin, J. S. (1996). "A damage mechanics model for compression strength of composites". Int. J. Solid Struct., 33 (29), 4379-4393.

Berbinau, P., Soutis, C., and Guz, I.A. (1999). "Compressive failure of 0° unidirectional carbon-fibre-reinforced plastic (CFRP) laminates by fibre microbuckling". Compos. Sci. Technol., 59, 1451-1455.

Budiansky, B. (1983). "Micro-mechanics". Computers and Structures, 16 (1-4), 3-12.

Budiansky, B., and Fleck, N. A. (1993). "Compressive failure of fiber composites". Journal of Mechanics and Physics of Solids, 41, 183-211.

Chen, X., Gupta, V., and Tian, J. (2006). "Mechanism-based failure laws for biaxially compressed IM7/8551-7 graphite–epoxy laminates". Journal of Composite Materials, 40 (10), 899-923.

Creighton, C. J., Sutcliffc, M. P., and Cylne, T. W. (2001). "A multiple field analysis procedure for characterization of fiber alignment in composites". Composites: Part A, 32, 221-229.

Fleck, N. A., and Budiansky, B. (1990). "Compressive failure of fiber composites due to micro-buckling. Inelastic deformation of composite materials". Dovark, G. J., Editor, Springer Verlag, 235-274.

Frost, S. R. (1992). "Compressive behavior of long fiber unidirectional composites". Journal of Composite Materials, 26 (8), 1151-1172.

Häberle, J. G., and Matthews, F. L. (1994). "A Micro-mechanics model for compression failure of unidirectional fiber-reinforced plastics". Journal of Composite Materials, (28), 1618-1639.

Huang, Z. M. (2001). "Micromechanical prediction of ultimate strength of transversely isotropic fibrous composites". International Journal of Solids and Structures, 28 (22-23), 4147-4172.

Huang, Z. M. (2001). "Simulation of the mechanical properties of fibrous composites by the bridging micromechanics model". Composites, Part A: Applied Science and Manufacturing, 32 (2), 143-172.

Jelf, P. M., and Fleck, N. A. (1992). "Compression failure mechanisms in unidirectional composites". Journal of Composite Materials, 26 (18), 2707-2726.

Jumahat, A., Soutis, C., and Hodzic, A. (2011). "A graphical method predicting the compressive strength of toughened unidirectional composite laminates". Applied Composite Materials, 18 (1), 65-83.

Karakuzu, R., Icten, B. M., and Tekinsen, Ö. (2010). "Failure behavior of composite laminates with multi-pin loaded holes". Journal of Reinforced Plastics and Composites, 29 (2), 247-253.

Mishra, A., and Naik, N. K. (2009). "Inverse micromechanical models for compressive strength of unidirectional composites". Journal of Composite Materials, 43 (10), 1199-1211.

Ranganathan, S., and Mantena, P. R. (2003). "Axial loading and buckling response characteristics of pultruded hybrid glass-graphite/epoxy composite beams". Journal of Reinforced Plastics and Composites, 22 (7), 671-679.

Rosen, B. W. (1965). "Mechanics of composite strengthening in fiber composite materials". American Society for Metals, Metals Park, Ohio, 37-75.

Soutis, C., and Fleck, N. A. (1990). "Static compression failure of fiber T800/924C composite plate with a single hole". Journal of Composite Materials, 24, 536-558.

Steif, P. S. (1990). "A model for kinking in fiber composites-I. Fiber breakage via micro-buckling". International Journal of Solids Structures, 26, 549-561.

Steif, P. S. (1990). "A model for kinking in fiber composites-II. Kink band formation". International Journal of Solids Structures, 26, 549-561.

Tomblin, J. S., and Barbero, E. J. (1996). "A damage mechanics model for compressive strength of fiber reinforced composites." ASTM Special Technical Publications STP J242, ASTM 13th Symposium on Composite Materials: Testing and Design, May 20-2 t, Orlando, FL.

Turgartis, S. W. (1987). "Measurement of small angle fiber misalignment in continuous fiber composites". Composite Science Technology, 30, 279-293.

Wisnom, M. R. (1990). "Effect of fiber misalignment on the compressive strength of unidirectional carbon fiber/Epoxy". Composites, 21 (5), 403-407.

Yeh, J. R., and Teply, J. L. (1988). "Compressive response of Kevlar/Epoxy composites". Journal of Composite Materials, 22, 245-257.